J|A|C|S
ARTICLES

Published on Web 06/15/2010

Iron-Catalyzed Hydrogen Production from Formic Acid

Albert Boddien,[†] Björn Loges,[†] Felix Gärtner,[†] Christian Torborg,[†] Koichi Fumino,[‡] Henrik Junge,[†] Ralf Ludwig,*[,†,‡] and Matthias Beller*[,†]

Leibniz - Institut für Katalyse e.V. an der Universität Rostock, Albert Einstein Str. 29a, Rostock, 18059, Germany and Universität Rostock, Institut für Chemie, Abteilung Physikalische Chemie, Dr. Lorenz Weg 1, Rostock, 18059, Germany

Received September 17, 2009; E-mail: matthias.beller@catalysis.de; ralf.ludwig@uni-rostock.de

Abstract: Hydrogen represents a clean energy source, which can be efficiently used in fuel cells generating electricity with water as the only byproduct. However, hydrogen generation from renewables under mild conditions and efficient hydrogen storage in a safe and reversible manner constitute important challenges. In this respect formic acid (HCO_2H) represents a convenient hydrogen storage material, because it is one of the major products from biomass and can undergo selective decomposition to hydrogen and carbon dioxide in the presence of suitable catalysts. Here, the first light-driven iron-based catalytic system for hydrogen generation from formic acid is reported. By application of a catalyst formed *in situ* from inexpensive $Fe_3(CO)_{12}$, 2,2′:6′2″-terpyridine or 1,10-phenanthroline, and triphenylphosphine, hydrogen generation is possible under visible light irradiation and ambient temperature. Depending on the kind of *N*-ligands significant catalyst turnover numbers (>100) and turnover frequencies (up to 200 h^{-1}) are observed, which are the highest known to date for nonprecious metal catalyzed hydrogen generation from formic acid. NMR, IR studies, and DFT calculations of iron complexes, which are formed under reaction conditions, confirm that PPh_3 plays an active role in the catalytic cycle and that *N*-ligands enhance the stability of the system. It is shown that the reaction mechanism includes iron hydride species which are generated exclusively under irradiation with visible light.

Introduction

Hydrogen has attracted considerable attention as an alternative clean energy vector. So far, hydrogen production via steam reforming and coal gasification is based to >95% on limited fossil resources such as coal and oil. On a mid- to long-term basis, there is an increasing demand for alternative technologies to generate hydrogen in a more sustainable manner.[1] The development of improved technologies for hydrogen generation and hydrogen storage in a safe and reversible manner is a prerequisite for the utilization of H_2 as transportation fuel.[2] Even though hydrogen generation from biomass like methanol, ethanol, or formic acid also involves the emission of the greenhouse gas CO_2, recycling is possible through photosynthesis in nature or technical processes in industry (CCS).[3] Notably, natural iron-based hydrogenases are known as highly efficient catalysts to produce hydrogen or utilize it as an energy source at ambient conditions. In this respect biomimetic hydrogen production, particularly employing sunlight and easily available non-noble metal catalysts, is a major challenge for science.[4] While iron-based enzymatic redox processes have been extensively studied in the past decades, only a few reduction reactions applying synthetic iron complexes, especially light-involving processes, are known today. This is in clear contradiction to the numerous examples of reduction processes in nature.[5]

Among the different hydrogen storage materials, formic acid (4.4 wt % hydrogen) has recently received considerable attention.[6] HCO_2H is one of the major products formed in biomass

[†] Leibniz - Institut für Katalyse e.V. an der Universität Rostock.
[‡] Universität Rostock, Institut für Chemie.

(1) (a) Turner, J. A. *Science* **2004**, *305*, 972. (b) Armaroli, N.; Balzani, V. *Angew. Chem., Int. Ed.* **2007**, *46*, 52. (c) Züttel, A.; Schlapbach, L. *Nature* **2001**, *414*, 353. (d) Armstrong, F. A.; Fontecilla-Camps, J. C. *Science* **2008**, *321*, 498. (e) Lubitz, W.; Tumas, W. *Chem. Rev.* **2007**, *107*, 3900.

(2) (a) Eberle, U.; Felderhoff, A.; Schüth, F. *Angew. Chem., Int. Ed.* **2009**, *48*, 6608. (b) Thomas, K. M. *Catal. Today* **2007**, *120*, 389. (c) van den Berg, A. W. C.; Areán, C. O. *Chem. Commun.* **2008**, 668. (d) Murray, L. J.; Dinca, M.; Long, J. R. *Chem. Soc. Rev.* **2009**, *38*, 1294. (e) Morris, R. E.; Wheatley, P. S. *Angew. Chem., Int. Ed.* **2008**, *47*, 4966. (f) Schüth, F.; Bogdanovic, B.; Felderhoff, M. *Chem. Commun.* **2004**, 2249. (g) Biniwale, R. B.; Rayalu, S.; Devotta, S.; Ichikawa, M. *Int. J. Hydrogen Energy* **2007**, *33*, 360. (h) Crabtree, R. H. *Energy Environ. Sci.* **2008**, *1*, 134. (i) Hu, Y. H.; Ruckenstein, E. *Ind. Eng. Chem. Res.* **2008**, *47*, 48. (j) Graetz, J. *Chem. Soc. Rev.* **2009**, *38*, 73. (k) Hamilton, C. W.; Baker, R. T.; Staubitz, A.; Manners, I. *Chem. Soc. Rev.* **2009**, *38*, 279. (l) Marrero-Alfonso, E. Y.; Beaird, A. M.; Davis, T. A.; Matthews, M. A. *Ind. Eng. Chem. Res.* **2009**, *48*, 3703. (m) Collins, D. J.; Zhou, H. C. *J. Mater. Chem.* **2007**, *17*, 3154.

(3) (a) Ntaikou, I; Gavala, H. N.; Kornaros, M.; Lyberatos, G. *Int. J. Hydrogen Energy* **2008**, *33*, 1153. (b) Haszeldine, S. R. *Science* **2009**, *325*, 1647. (c) *Energy technology perspectives*; International Energy Agency: Paris, 2008 (www.iea.org).

(4) (a) Okura, I. *Coord. Chem. Rev.* **1985**, *68*, 53. (b) Lubitz, W.; Reijerse, E. J.; Messinger, J. *Energy Environ. Sci.* **2008**, *1*, 15. (c) Wang, M.; Yong, N.; Gorlov, M.; Sun, L. *Dalton Trans.* **2009**, 6458. (d) Fukuzumi, S. *Eur. J. Inorg. Chem.* **2008**, *9*, 1351. (e) Gärtner, F.; Sundararaju, B.; Surkus, A.-E.; Boddien, A.; Loges, B.; Junge, H.; Dixneuf, P. H.; Beller, M. *Angew. Chem., Int. Ed.* **2009**, *48*, 9962.

(5) (a) Enthaler, S.; Junge, K.; Beller, M. in *Iron Catalysis in Organic Chemistry*; Plietker, B., Ed.; Wiley-VCH: Weinheim, 2008. (b) Bolm, C.; Legros, J.; Le Paih, J.; Zani, L. *Chem. Rev.* **2004**, *104*, 6217. (c) Bitterwolf, T. E. *Coord. Chem. Rev.* **2006**, *250*, 388. (d) Fürstner, A.; Martin, R. *Chem. Lett.* **2005**, *34*, 624.

(6) (a) Enthaler, S. *ChemSusChem* **2008**, *1*, 801. (b) Joó, F. *ChemSusChem* **2008**, *1*, 805.

 10.1021/ja100925n

Figure 1. Hydrogen generation from biomass via formic acid as an intermediate compound.

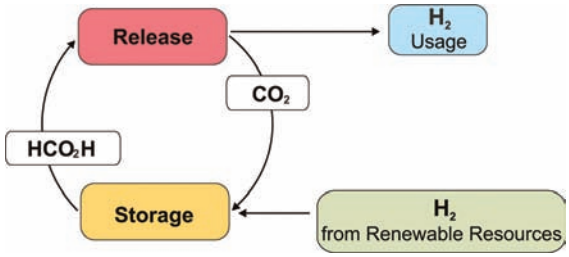

Figure 2. Hydrogen storage via carbon dioxide−formic acid conversion.

Scheme 1. Formic Acid Decomposition Pathways and Their Thermodynamic Properties[9c,10]

				ΔG° /kJ·mol⁻¹	ΔH° /kJ·mol⁻¹	ΔS° /J·mol⁻¹·K⁻¹
Eq. 1 :	dehydrogenation	HCO_2H	$\longrightarrow$ $CO_2 + H_2$	-32.9	31.2	215
Eq. 2 :	dehydration	HCO_2H	$\longrightarrow$ $CO + H_2O$	-12.4	28.7	138

processing such as fermentation, pyrolysis, and supercritical reactions and can undergo selective decomposition to hydrogen and carbon dioxide only in the presence of a catalyst (Figure 1).[7] In addition to hydrogen generation, a sustainable and reversible energy storage cycle can be envisioned by storage of hydrogen in formic acid and release from it (Figure 2). Here, carbon dioxide is converted to formic acid or formate derivatives either electrochemically[8] or by catalytic hydrogenation.[9] The resulting products are liquid at ambient conditions and can thus be handled, stored, and transported easily.

In general, formic acid and formates can be decomposed via dehydrogenation (eq 1) and dehydration (eq 2) pathways (Scheme 1). For the subsequent conversion of hydrogen into electrical energy the latter pathway has to be avoided, because fuel cells, especially proton exchange membrane fuel cells, do not tolerate carbon monoxide impurities.

Several heterogeneous[11] and homogeneous[12,13] catalyst systems for hydrogen release from HCO_2H have been studied since the beginning of the 20th century, and remarkable results have been reported in recent years. In 1998, Puddephat et al. studied the binuclear ruthenium phosphine complex $[Ru_2(\mu\text{-CO})(CO)_4(\mu\text{-dppm})_2]$ for selective hydrogen generation from formic acid. They achieved with their system at room temperature a turnover frequency (TOF = mol H_2/mol catalyst·h^{-1}) of ~500 h^{-1} after 15 min and full conversion.[14] In 2008, Fukuzumi and co-workers investigated $[Rh(Cp^*)(bipy)-(H_2O)](SO_4)$ and similar complexes for the hydrogen generation from aqueous formic acid solutions. They demonstrated that formic acid decomposition occurs via formate and a hydride complex.[15] More recently, this group demonstrated that heteronuclear iridium−ruthenium complexes are highly active catalysts for hydrogen generation in an aqueous solution under ambient conditions giving a TOF of ~426 h^{-1}.[15b] Himeda et al. focused on iridium complexes for hydrogen generation from formic acid/sodium formate in aqueous solution and achieved an initial TOF of 14 000 h^{-1} at 90 °C.[16] Our group and Laurenczy et al. independently demonstrated that hydrogen generation is also possible under relatively mild conditions using ruthenium phosphine complexes.[17] We identified several ruthenium phosphine complexes which are capable of generating hydrogen from formic acid amine adducts selectively at room temperature.[18] The catalyst activity is strongly influenced by the nature and the concentration of amine in solution, which is not consumed during the reaction and can easily be recovered from the reaction solution after full conversion.[19] An active catalyst system containing *N*,*N*-dimethylhexylamine, $[RuCl_2(benzene)]_2$, and 1,2-bis(diphenylphosphino)ethane (dppe) was investigated in both batch and continuous mode and reached at room temperature a turnover number (TON = mol of H_2/mol of catalyst) of more than 260 000 with a TOF of 900 h^{-1}, which is the highest activity for hydrogen generation from formic acid.[20] Most recently, we

(7) (a) Reunanen, J.; Oinas, P.; Nissinen, T. A process for recovery of formic acid. PCT Int. Appl., 2009. (b) Kruse, A.; Gawlik, A. *Ind. Eng. Chem. Res.* **2003**, *42*, 267. (c) Hayes, D. J.; Fitzpatrick, S.; Hayes, M. H. B.; Ross, J. R. H. in *Biorefineries-Industrial Processes and Products*; Kamm, B.; Gruber, P. R., Kamm, M., Ed.; Wiley-VCH, Weinheim, 2006; p 139.

(8) (a) Benson, E. E.; Kubiak, C. P.; Sathrum, A. J.; Smieja, J. M. *Chem. Soc. Rev.* **2009**, *38*, 89. (b) Marks, J. T. et al. *Chem. Rev.* **2001**, *101*, 953.

(9) (a) Leitner, W. *Angew. Chem., Int. Ed. Engl.* **1995**, *34*, 2207. (b) Jessop, P. G.; Joó, F.; Tai, C. C. *Coord. Chem. Rev.* **2004**, *248*, 2425. (c) Jessop, P. G. in *The Handbook of Homogeneous Hydrogenation*; de Vries, J. G., Elsevier, C. J., Eds.; Wiley-VCH: Weinheim, 2007; p 489.

(10) NIST Chemistry Webbook. http://webbook.nist.gov (accessed 24.08. 2009).

(11) (a) Rienäcker, G.; Mueller, H. *Z. Anorg. Allg. Chem.* **1968**, *357*, 255. (b) Garcia-Verdugo, E.; Liu, Z.; Ramirez, E.; Garcia-Serna, J.; Fraga-Dubreuil, J.; Hyde, J. R.; Hamley, P. A.; Poliakoff, M. *Green Chem.* **2006**, *8*, 359. (c) Hyde, J. R.; Poliakoff, M. *Chem. Commun.* **2004**, 1482. (d) Hyde, J. R.; Walsh, B.; Singh, J.; Poliakoff, M. *Green Chem.* **2005**, *7*, 357. (e) Wiener, H.; Sasson, Y.; Blum, J. *J. Mol. Catal.* **1986**, *35*, 277. (f) Zhou, X.; Huang, Y.; Xing, W.; Liu, C.; Liao, J.; Lu, T. *Chem. Commun.* **2008**, 3540. (g) Ojeda, M.; Iglesia, E. *Angew. Chem., Int. Ed.* **2009**, *48*, 4800. (h) Kiliç, E. Ö; Koparal, A. S.; Ögütveren, Ü. B. *Fuel Proc. Technol.* **2009**, *90*, 158. (i) Sun, B.; Smirniotis, P. G. *Catal. Today* **2003**, *88*, 49. (j) Kakuta, S.; Toshiyuki, A. *Appl. Mater. Interfaces* **2009**, *1*, 2707.

(12) For an exellent review see: (a) Johnson, C. T.; Morris, D. J.; Wills, M. *Chem. Soc. Rev.* **2010**, *39*, 81. (b) Loges, B.; Boddien, A.; Gärtner, F.; Junge, H.; Beller, M. *Top. Catal.* **2010**, DOI: 10.1007/s11244-010-9522-8.

(13) (a) Coffey, R. S. *Chem. Commun.* **1967**, *18*, 923. (b) Forster, D.; Beck, G. R. *Chem. Commun.* **1971**, *994*, 1072. (c) Laine, R. M.; Rinker, R. G.; Ford, P. C. *J. Am. Chem. Soc.* **1977**, *99*, 252. (d) Yoshida, T.; Ueda, Y.; Otsuka, S. *J. Am. Chem. Soc.* **1978**, *100*, 3941. (e) Strauss, S. H.; Whitmire, K. H.; Shriver, D. F. *J. Organomet. Chem.* **1979**, *174*, C59. (f) Paonessa, R. S.; Trogler, W. C. *J. Am. Chem. Soc.* **1982**, *104*, 3529. (g) King, R. B.; Bhattacharyya, N. K. *Inorg. Chim. Acta* **1995**, *237*, 65. (h) Man, M. L.; Zhou, Z.; Ng, S. M.; Lau, C. P. *Dalton Trans.* **2003**, 3727.

(14) (a) Gao, Y.; Kuncheria, J.; Yap, G. P. A.; Puddephatt, R. J. *Chem. Commun.* **1998**, 2365. (b) Gao, Y.; Kuncheria, J. K.; Jenkins, H. A.; Puddephatt, R. J.; Yap, G. P. A. *J. Chem. Soc., Dalton Trans.* **2000**, 3212. (c) Shin, J. H.; Churchill, D. G.; Parkin, G. *J. Organomet. Chem.* **2002**, *642*, 9.

(15) (a) Fukuzumi, S.; Kobayashi, T.; Suenobu, T. *ChemSusChem* **2008**, *1*, 827. (b) Fukuzumi, S.; Kobayashi, T.; Suenobu, T. *J. Am. Chem. Soc.* **2010**, *132*, 1496.

(16) Himeda, Y. *Green Chem.* **2009**, *11*, 2018.

(17) (a) Fellay, C.; Yan, N.; Dyson, P. J.; Laurenczy, G. *Chem.—Eur. J.* **2009**, *15*, 3752. (b) Gan, W.; Dyson, P. J.; Laurenczy, G. *React. Kinet. Catal. Lett.* **2009**, *89*, 205. (c) Loges, B.; Boddien, A.; Junge, H.; Beller, M. *Angew. Chem., Int. Ed.* **2008**, *47*, 3962. (d) Fellay, C.; Dyson, P. J.; Laurenczy, G. *Angew. Chem., Int. Ed.* **2008**, *47*, 3966.

(18) Boddien, A.; Loges, B.; Junge, H.; Beller, M. *ChemSusChem* **2008**, *1*, 751.

(19) Junge, H.; Boddien, A.; Capitta, F.; Loges, B.; Noyes, J. R.; Gladiali, S.; Beller, M. *Tetrahedron Lett.* **2009**, *50*, 1603.

(20) Boddien, A.; Loges, B.; Junge, H.; Gärtner, F.; Noyes, J. R.; Beller, M. *Adv. Synth. Catal.* **2009**, *351*, 2517.

showed that ruthenium phosphine catalyst systems can be triggered and accelerated via irradiation with visible light.[21]

An actual goal in organometallic catalysis is the replacement of noble metal-based catalysts, such as ruthenium, iridium, palladium, and rhodium, with nonprecious metal catalysts such as iron compounds.[22,23] *Until now, no homogeneous non-noble metal catalyst system is known for selective hydrogen generation from formic acid under ambient conditions.*[24,25] Herein, we report that simple iron carbonyl phosphine complexes allow for this transformation in the presence of visible light.

Results and Discussion

Catalyst Design. We started our investigation with an initial catalyst testing of numerous non-noble metal precursors in combination with different phosphorus and nitrogen containing ligands. For this purpose we applied the convenient method of Jessop et al. who used a visual dye based assay screening to discover potential catalysts suitable for hydrogenation of carbon dioxide to formic acid.[26] We adopted this method, using pressure tubes with valves as assays and the acid−base indicator bromthymol blue to identify promising candidates, for hydrogen generation from formic acid (see Supporting Information).[27] To ensure that the indicator does not influence catalysis it was added after the reaction was finished. The color change of the indicator from yellow to blue takes place at a ratio of 2.08 to 1.47 of formic acid/1,8-diazabicyclo[5.4.0]undec-7-ene (DBU) in DMSO. In general, the reactions were performed with 60 μmol of catalyst in DMSO in 1 mL of formic acid/DBU mixture (5:3) at 60−120 °C for 24−72 h under an inert gas atmosphere (argon). Organometallic precursors including Cr, Mn, Fe, Co, Ni, Cu, and Mo-compounds together with different *P*- and *N*-ligands were tested, and suitable candidates identified. All reactions which showed color changes were tested again using a procedure with a quantitative and qualitative determination of the evolved gases. In such a standard experiment a double-walled thermostatically controlled reaction vessel was evacuated, heated, and purged with argon 10 times to remove any other gases. The metal complexes (60 μmol of metal) and ligands (mostly 1 equiv) were added either as powders in a Teflon crucible and 1 mL of solvent or from a freshly prepared stock solution (1 mL). A 5 mL aliquot of $5HCO_2H \cdot 2NEt_3$ (FA/TEA) was placed in the vessel, and the desired temperature was kept constant. The reactions were started after equilibration for at least 30 min. The volume of evolved gases was quantitatively measured using automatic gas burets.[18,28] In addition, gases were qualitatively and quantitatively determined by GC (gas chromatograph HP6890N, carboxen 1000, TCD, external calibration). The conversion of formic acid in general did not exceed 10%.

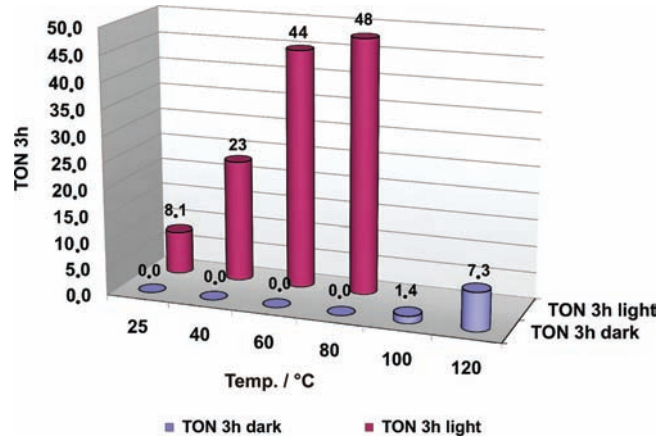

Figure 3. TON of HCO_2H decomposition using 20 μmol of $Fe_3(CO)_{12}$/PPh_3/tpy (Fe/PPh_3/tpy 1:1:1) in 5 mL of $5HCO_2H \cdot 2NEt_3$ + 1 mL of DMF, ambient pressure, reaction time 3 h, light source (Xenon lamp 300 W, 385 nm cutoff via hot mirror).

The best catalyst system identified was triirondodecacarbonyl ($Fe_3(CO)_{12}$) in the presence of triphenylphosphine (PPh_3), 2,2′:6′2″-terpyridine (tpy), and dimethylformamide (DMF). This system was capable of generating hydrogen from formic acid amine adducts at temperatures above 100 °C, whereas significant gas evolution occurred at 120 °C (Figure 3, blue column). Unfortunately, the selectivity of the thermal reaction is very low (H_2 or CO_2/CO 1:5), showing that dehydration is favored at higher temperatures.

However, by testing the *in situ* generated catalyst system under visible light irradiation hydrogen generation even occurred at room temperature (Figure 3)! The light source which was used for irradiation was a 300 W PerkinElmer Cermax PE300BF Xenon Arc lamp. An A2-005 hot mirror was employed as a filter to remove the UV portion (<385 nm) and IR portion (>750 nm) of the light spectrum. Irradiation of the solution with visible light exclusively led to dehydrogenation, and only traces of CO were detected via GC analysis. The catalyst activity increased gradually between 25−60 °C and leveled off at ∼80 °C (Figure 3, red column).

Additionally we tested also other metal carbonyl complexes in low oxidation states to determine whether similar effects upon irradiation can be observed. All reactions shown in Table 1 were performed at ambient temperature (40 °C), in DMF, and in the presence of 60 μmol of metal following our standard protocol. In cases where significant gas evolution occurred, the gas mixtures contained H_2:CO_2 (1:1) and only traces of CO.

Reactions with molybdenumhexacarbonyl ($Mo(CO)_6$) and dimanganesedecacarbonyl ($Mn_2(CO)_{10}$) gave only slight activity

(21) Loges, B.; Boddien, A.; Noyes, J. R.; Baumann, W.; Junge, H.; Beller, M. *Chem. Commun.* **2009**, *28*, 4185.
(22) For recent reviews and highlights on iron catalysis, see: (a) Plietker, B., Ed. in *Iron Catalysis in Organic Chemistry*; Wiley-VCH: Weinheim, 2008. (b) Enthaler, S.; Junge, K.; Beller, M. *Angew. Chem., Int. Ed.* **2008**, *47*, 3317. (c) Gaillard, S.; Renaud, J.-L. *ChemSusChem* **2008**, *1*, 505. (d) Bolm, C.; Legros, J.; Paith, J. L.; Zani, L. *Chem. Rev.* **2004**, *104*, 6217. (e) Correa, A.; Mancheño, O. G.; Bolm, C. *Chem. Soc. Rev.* **2008**, *37*, 1108. (f) Sherry, B. D.; Fürstner, A. *Acc. Chem. Res.* **2008**, *41*, 1500. (g) Fürstner, A. *Angew. Chem., Int. Ed.* **2009**, *48*, 1364. (h) Bullock, R. M. *Angew. Chem., Int. Ed.* **2007**, *46*, 7360.
(23) Selected examples from our group: (a) Anilkumar, G.; Bitterlich, B.; Gelalcha, F. G.; Tse, M. K.; Beller, M. *Chem. Commun.* **2007**, 289. (b) Gelalcha, F. G.; Bitterlich, B.; Anilkumar, G.; Tse, M. K.; Beller, M. *Angew. Chem., Int. Ed.* **2007**, *46*, 7293. (c) Shi, F.; Tse, M. K.; Pohl, M.-M.; Brückner, A.; Zhang, S.; Beller, M. *Angew. Chem., Int. Ed* **2007**, *46*, 8866. (d) Kischel, J.; Jovel, I.; Mertins, K.; Zapf, A.; Beller, M. *Org. Lett.* **2006**, *8*, 19. (e) Iovel, I.; Mertins, K.; Kischel, J.; Zapf, A.; Beller, M. *Angew. Chem., Int. Ed.* **2005**, *44*, 3913.
(24) In this regard the current work of Wills et al. should be noted, who demonstrated recently the decomposition of formic acid in the presence of Fe(II) and Fe(III) catalysts at 120 °C with a turnover number (TON) of 3.
(25) Morris, D. J.; Clarkson, G. J.; Wills, M. *Organometallics* **2009**, *28*, 4133.
(26) Tai, C.-C.; Chang, T; Roller, B.; Jessop, P. G. *Inorg. Chem.* **2003**, *42*, 7340.
(27) Usage of the described pressure tube: (a) Hamid, M. H. S. A.; Allen, C. L.; Lamb, G. W.; Maxwell, A. C.; Maytum, H. C.; Watson, A. J. A.; Williams, J. M. J *J. Am. Chem. Soc.* **2009**, *131*, 1766.
(28) Loges, B.; Junge, H.; Spilker, B.; Fischer, C.; Beller, M. *Chem. Ing. Tech.* **2007**, *79*, 741.

Table 1. Activity of Different Non-Noble Metal Carbonyl Complexes[a]

$$HCO_2H \bullet \text{amine} \xrightarrow[40°C]{\text{catalyst}\ h\cdot\nu} H_2 + CO_2 + \text{amine}$$

entry	metal precursor	V2h/mL	V3h/mL	TON2h	TON3h
1	$Mo(CO)_6$	3.5	4.4	1.2	1.5
2	$Mn_2(CO)_{10}$	5.9	6.2	2.0	2.1
3[b]	$Cr(CO)_6$	1.3	1.5	–	–
4[b]	$Co_2(CO)_8$	1.6	1.8	–	–
5	$Fe(CO)_5$	32	41	11	14
6	$Fe_2(CO)_9$	44	59	15	20
7	$Fe_3(CO)_{12}$	50	68	17	23
8	$Fe(CO)_3$COT	29	38	9.8	13
9	$Fe(CO)_3$BDA[c]	44	56	15	19
10	$[CpFe(CO)_2]_2$	4.7	5.3	1.6	1.8

[a] Reaction conditions: 60 μmol of [M], PPh_3, tpy (Fe/PPh_3/tpy 1:1:1), 1 mL DMF, 5 mL $5HCO_2H\cdot 2NEt_3$, light irradiation via 300 W xenon lamp (385 nm cutoff via hot mirror), reaction time 3 h, gas measured via automatic gas buret and analyzed via GC (H_2/CO_2 1:1). [b] Neither H_2 nor CO_2 detected. [c] BDA = benzylideneacetone; the complex was synthesized according to Lewis or Brookhart.[29]

Table 2. Dependence of Catalytic Activity on the Ligand Combination PPh_3, tpy, and the Presence of Amine[a]

entry	ligand a	ligand b	V3h [mL]	TON3h
1	tpy	–	1.9	–
2	–	PPh_3	16	5.4
3	tpy	PPh_3	68 (131)[b]	23 (44)[b]
4[c]	tpy	PPh_3	5.6	1.9

[a] Reaction conditions: 20 μmol of $Fe_3(CO)_{12}$, PPh_3, tpy (Fe/PPh_3/tpy 1:1:1), 1 mL DMF, 5 mL $5HCO_2H\cdot 2NEt_3$, 40 °C, light irradiation via 300 W xenon lamp (385 nm cutoff via hot mirror), 3 h reaction time, gas measured via automatic gas buret and analyzed via GC (H_2/CO_2 1:1). [b] 24 h. [c] Without amine.

(Table 1, entries 1,2) under ambient conditions. In the presence of chromiumhexacarbonyl ($Cr(CO)_6$) and dicobaltoctacarbonyl ($Co_2(CO)_8$) no activity at all is observed (Table 1, entries 3, 4). In addition to $Fe_3(CO)_{12}$ other iron carbonyl complexes showed significant activity. For example, ironpentacarbonyl ($Fe(CO)_5$) and irontricarbonylcyclooctatetraene ($Fe(CO)_3$COT) showed comparable activity (Table 1, entries 5, 8). Higher activity is provided by diironnonacarbonyl ($Fe_2(CO)_9$) and irontricarbonylbenzylidenacetone ($Fe(CO)_3$BDA), whereas the highest TON of 23 after 3 h is achieved with $Fe_3(CO)_{12}$ as a precatalyst (Table 1, entries 6, 7, 9). To identify the influence of the different ligands on the catalytic system we performed reactions at 40 °C under irradiation with only one type of ligand present. Moreover, the reaction was performed without amine present (Table 2).

While $Fe_3(CO)_{12}$ with 3 equiv of tpy (Fe/tpy 1:1) showed almost no activity, significant hydrogen evolution occurred with 3 equiv of PPh_3 (Fe/PPh_3 1:1) (Table 2, entries 1, 2). However, in the presence of a catalyst system containing Fe/tpy/PPh_3 (ratio 1:1:1) under irradiation a significant higher activity is obtained, resulting in a TON of 44 (Table 2, entry 3) after 24 h. The absence of amine resulted in very low activity (Table 2, entry 4).

Light Effects. As shown above hydrogen generation from formic acid in the presence of iron carbonyl complexes strongly depends on light irradiation. UV/vis experiments (Lambda 5, Perkin-Elmer) of the reaction solution ($Fe_3(CO)_{12}$/3tpy/3PPh_3 in $5HCO_2H\cdot 2NEt_3$ and DMF) revealed absorbance at 276.6, 283.8, and 320.2 nm in the UV region and 555.6 nm in the visible light region, which is shown in Figure 4.

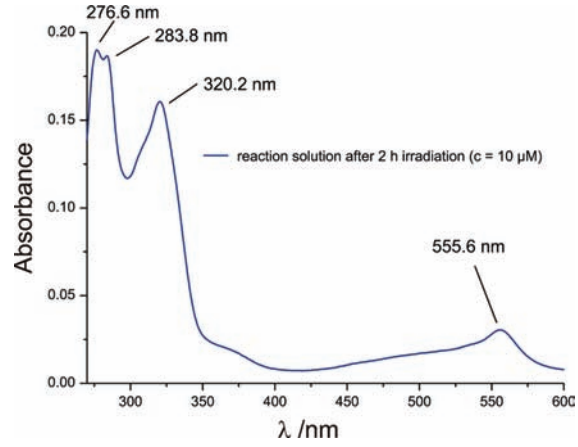

Figure 4. UV/vis spectrum of $Fe_3(CO)_{12}$ + 3 equiv of PPh_3 + 3 equiv of tpy (Fe/PPh_3/tpy 1:1:1) in DMF and $5HCO_2H\cdot 2NEt_3$ after 2 h of visible light irradiation.

To distinguish between photoinduced and photoassisted reactions we performed experiments where light is turned on and off during constant time intervals (Figure 5). To minimize temperature effects during these switches we performed the reaction at 60 °C. The gas volume was quantified via gas buret, and the hydrogen content was analyzed online using a hydrogen sensor (Hach Ultra Analytics GmbH) and GC after the reaction.

During the first 5 min in the absence of light, only a slight volume increase is observed, caused by interferences of the equilibrium during the start. Then, irradiation with visible light generated, through a photoinduced effect, an active iron catalyst system and hydrogen production started. The average reaction rate within the first and the second light period was 1 $mL\cdot min^{-1}$ and decreased during the following switches to 0.5 $mL\cdot min^{-1}$. In the first 5 min of each light period, the reaction rate reached a maximum which is explained by an initial volume increase due to an initial temperature increase, according to a small heat transfer from the lamp. This is not the case under constant irradiation in standard experiments. The equilibrium is reached within a short time by the thermostat. Figure 5 shows clearly that without irradiation no gas evolution is observed; therefore light is essential to generate an active catalyst. *Moreover, when light irradiation is stopped, gas evolution breaks down immediately, which unambiguously indicates that light not only is responsible for generating an active system but also drives the catalytic cycle!* Therefore, we assume a photoassisted hydrogen generation.

Ligand Effects: Influence of Different *P*- and *N*-Ligands. To improve the catalyst system a variety of phosphine and phosphite ligands with different electronic and steric properties have been investigated for their ability to promote hydrogen generation from formic acid in the presence of $Fe_3(CO)_{12}$ and 3 equiv of tpy (Fe/tpy 1:1) in DMF at 40 or 60 °C (Figure 6).

Among the phosphine ligands tested at 40 °C, bidentate ligands like 1,2-bis(diphenylphosphino)methane (dppm) and 1,2-bis(diphenylphosphino)ethane (dppe) showed only very low activity. Standard ligands such as PPh_3 or PCy_3 provided higher activity. Hence, a number of monodentate *P*-ligands were tested at 60 °C. Tris(4-fluoromethylphenyl)phosphine (**1**), tris(4-methoxyphenyl)phosphine (**3**), and tris(2-furyl)phosphine (**4**)

(29) (a) Domingos, A. J. P.; Howell, J. A. S.; Johnson, B. F. G.; Lewis, J. *Inorg. Synth.* **1976**, *16*, 103. (b) Brookhart, M.; Nelson, G. O. *J. Organomet. Chem.* **1979**, *164*, 193.

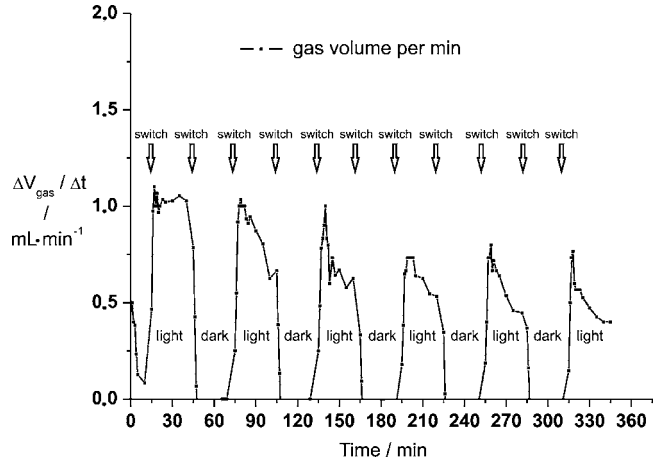

Figure 5. The light switch experiment was performed with $Fe_3(CO)_{12}$ (20 μmol) + 3 equiv of PPh_3 + 3 equiv of tpy (Fe/PPh_3/tpy 1:1:1) in DMF (1 mL) and $5HCO_2H \cdot 2NEt_3$ (5 mL). After a 15 min induction period, the light source (300 W xenon lamp; 385 nm cutoff via hot mirror) was switched on and off every 30 min. Gas measured via gas buret and analyzed by GC and online via H_2-sensor (H_2/CO_2 1:1).

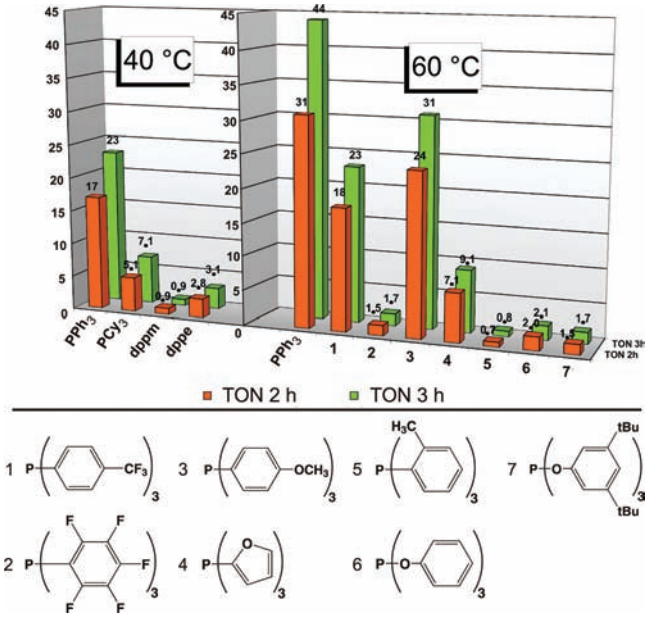

Figure 6. Influence of different phosphine and phosphite ligands on the activity (TON) of H_2 generation from HCO_2H using 20 μmol of $Fe_3(CO)_{12}$/*P*-ligand/tpy (Fe/P/tpy 1:1:1) in 5 mL of $5HCO_2H \cdot 2NEt_3$, 1 mL of DMF, ambient pressure, reaction time 3 h, light irradiation via 300 W xenon lamp (385 nm cutoff via hot mirror).

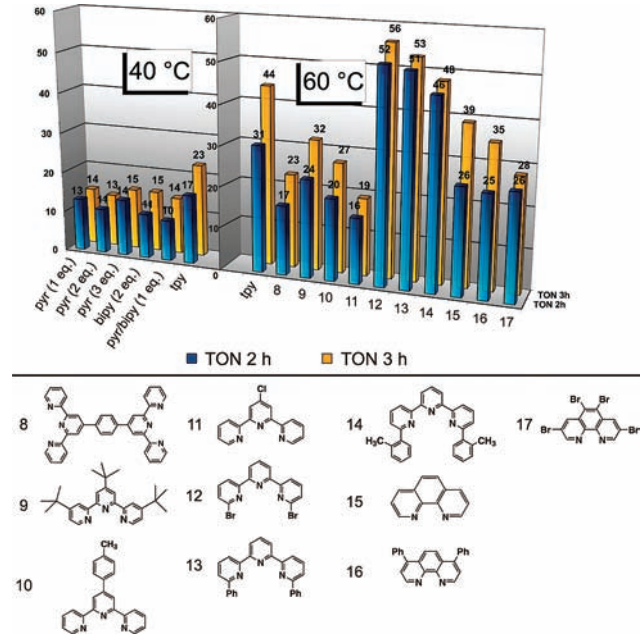

Figure 7. Influence of different nitrogen containing ligands on the activity (TON) of H_2 generation from HCO_2H using 20 μmol of $Fe_3(CO)_{12}$/PPh_3/ligand (Fe/PPh_3/ligand 1:1:1) in 5 mL of $5HCO_2H \cdot 2NEt_3$ + 1 mL of DMF, ambient pressure, reaction time 3 h, light irradiation via 300 W xenon lamp (385 nm cutoff via hot mirror).

showed significant activity. On the other hand tris(pentafluorophenyl)phosphine (**2**), tris(2-tolyl)phosphine (**5**), and phosphite ligands triphenylphosphite (**6**) and tris(3,5-tertbutyl)phosphite (**7**) gave only negligible activities. In addition, we also examined different *N*-ligands, e.g. pyridine (pyr), bipyridine (bipy), terpyridine, and phenanthroline derivatives, to obtain a stable and active catalyst system (Figure 7).

Applying bipyridine or pyridine resulted in a slightly lower activity. However, varying the amount of pyridine from Fe/pyridine = 1:1 to Fe/pyridine 1:3 had no influence on the catalyst activity. Interestingly, usage of 2 equiv of bipy (Fe/bipy 1:2) or 1 equiv of pyr/bipy (Fe/pyridine/bipy 1:1:1) provided similar turnover numbers. A significant influence on the catalyst activity is observed using different terpyridine and phenanthroline ligands at 60 °C. For example, 4′,4‴′-(1,4-phenylene)bis(2,2′:6′,2″-terpyridine) (**8**), bearing two terpyridine moieties being connected via a phenyl bridge, inhibited catalysis. Also 4,4′,4″-(tri-*tert*-butyl)-2,2′:6′,2″-terpyridine (**9**), 4′-(4-methylphenyl)-2,2′:6′,2″-terpyridine (**10**), and 4′-(chloro)-2,2′:6′,2″-terpyridine (**11**) gave lower activities compared to terpyridine itself. Interestingly, when changing the substituent in the 6,6″-positions of terpyridine from H to bromine, phenyl, or 2-methylphenyl groups, an increase of activity is observed. 6,6″-(Bromo)-2,2′:6′,2″-terpyridine (**12**) and 6,6″-(phenyl)-2,2′:6′,2″-terpyridine (**13**) provided the highest activity with a turnover frequency (TOF) of 200 h^{-1} for **13** compared to 84 h^{-1} for terpyridine. However, the catalyst system derived from terpyridine provided a longer time stability. Among the tested phenanthroline coligands 1,10-phenanthroline (phen) (**15**) and 4,7-diphenyl-1,10-phenanthroline (**16**) led to high activity which was comparable to the terpyridine system after 3 h, whereas in the presence of 3,5,6,8-tetrabromo-1,10-phenathroline (**17**) a considerable lower activity and stability were observed. After

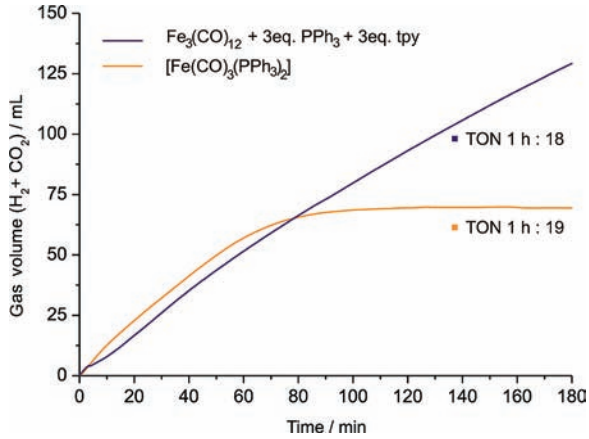

Figure 8. Comparison of the catalyst activity of the *in situ* generated catalyst from $Fe_3(CO)_{12}$/PPh_3/tpy and $[Fe(CO)_3(PPh_3)_2]$ for H_2 generation from HCO_2H using 20 μmol of $Fe_3(CO)_{12}$/PPh_3/tpy (Fe/PPh_3/tpy 1:1:1) and 60 μmol of $[Fe(CO)_3(PPh_3)_2]$ in 5 mL of $5HCO_2H{\cdot}2NEt_3$ + 1 mL of DMF, ambient pressure, 60 °C, reaction time 3 h, light irradiation via 300 W xenon lamp (385 nm cutoff via hot mirror).

24 h **15** gave a turnover number of 126 underlining the stability of these catalyst systems. *Notably, this is the highest catalyst productivity known for any homogeneous hydrogen generation from formic acid with non-noble metal complexes*. In summary, it was found that both *P*- and *N*-ligands have a significant influence on the activity and stability of the catalytic system. Within the tested *P*-ligands PPh_3 gave the best activity; a direct dependence of the activity on the electronic and steric properties of the *N*- and *P*-ligands was not observed. Among the investigated *N*-ligands 6,6″-substituted terpyridine ligands led to high activity but lower stability. Phenanthroline ligands provided a longer stability.

Spectroscopic Insight and Computational Analysis of Iron-Catalyzed Hydrogen Generation from Formic Acid. To identify active catalyst species, MS and HRMS studies applying ESI-TOF (see Supporting Information) of the reaction mixture containing $Fe_3(CO)_{12}$, 3 equiv of PPh_3, and 3 equiv of tpy (Fe/P/tpy 1:1:1) were performed. Here, $[HFe(CO)(PPh_3)(tpy)]^-$ (580 *m*/*z*) and $[Fe(CO)_3(PPh_3)_2]$ (664 *m*/*z*) were detected as the two main iron species. To isolate these complexes $[Fe(CO)_3(PPh_3)_2]$ was synthesized according to a modified literature protocol,[30] while attempts to prepare $[Fe(CO)(PPh_3)(tpy)]$ and $[HFe(CO)(PPh_3)(tpy)]^-$ failed. Next, we tested the defined complex $[Fe(CO)_3(PPh_3)_2]$ for hydrogen generation (Figure 8) and compared the catalyst activity to the *in situ* system with $Fe_3(CO)_{12}$/PPh_3/tpy.

Notably, the reaction rates for the *in situ* catalyst system and the defined complex were comparable within the first hour confirming the same active species. Then, the molecular defined precatalyst $[Fe(CO)_3(PPh_3)_2]$ is rapidly deactivated, which is not the case for the *in situ* catalyst mixture, where terpyridine is included. Apparently, in the *in situ* catalyst mixture terpyridine is needed only for stabilizing purposes.

Both catalyst systems were also studied by NMR and IR spectroscopy. ^1H and ^{31}P NMR studies (295 K, 300 MHz) were performed in DMF-d_7 simulating the reaction conditions. In Figure 9, the ^{31}P NMR spectra of both the *in situ* catalyst and $[Fe(CO)_3(PPh_3)_2]$ under the same reaction conditions ($5HCO_2H{\cdot}2NEt_3$; irradiation) are shown.

The ^{31}P NMR spectrum of the *in situ* mixture without irradiation (FA/TEA present) exhibited two main singlets at 70.6 and 82.5 ppm (ratio 7/1) after the ligands were introduced, which indicated that PPh_3 is coordinated to the metal center forming two complexes. Additionally, small singlets at 25.58 and −5.4 ppm, which correspond to impurities of triphenylphosphineoxide and free triphenylphosphine, respectively, are observed. $[Fe(CO)_3(PPh_3)_2]$ in DMF with FA/TEA showed only one singlet at 82.7 ppm, which corresponds to two equally bonded triphenylphosphine ligands (Figure 9A).[31] Thus, formation of $[Fe(CO)_3(PPh_3)_2]$ in the *in situ* catalyst mixture is confirmed by ^{31}P NMR. After irradiation of this solution for 10 min two singlets at 70.6 and 82.5 ppm and free PPh_3 at −5.4 ppm (3/1/2) are observed in the ^{31}P NMR spectrum. At the same time in the ^1H NMR spectrum a signal is formed at −8.9 ppm, which proved the formation of an iron hydride species. This proton shift is within the same range as those reported for other monomolecular Fe−H species.[32]

The reaction solution containing $[Fe(CO)_3(PPh_3)_2]$ showed four singlets in the ^{31}P spectrum after 10 min of irradiation. The signal at 82.7 decreased, and two new complexes are formed with signals at 80.6 and 70.8 ppm (49/10/1). The signal at 70.8 ppm corresponds to a hydride signal at −8.8 (s) ppm, whereas the signal at 80.6 corresponds to a triplet at −9.1 ppm, which cannot be observed in the *in situ* catalyst mixture in the presence of terpyridine (Figure 9B). It is important to note that all hydride signals are only observed when the reaction solutions were irradiated! After 30 min of irradiation the ratio of the signals at 82.5 to 70.6 ppm of the *in situ* catalyst mixture reached 1:1 (Figure 9C) and the ratio of bonded phosphine to free PPh_3 decreased from 5:1 (Figure 9A) to 2:1 (Figure 9C). Irradiating the $[Fe(CO)_3(PPh_3)_2]$ solution for 30 min led to a ratio of the signals at 82.7, 80.6, and 70.8 ppm of 15/6/1. Here, the signal of bonded triphenylphosphine to free PPh_3 decreased during 30 min of irradiation from 17:1 (Figure 9A) to 3:2 (Figure 9C). The ratio of hydride signals at −9.1 (t) and −8.8 (s) ppm were in the same range like the phosphorus signals 80.6 and 70.8 ppm (Figure 9, C). From the NMR studies it can be concluded that, in both reaction mixtures, besides other complexes, $[Fe(CO)_3(PPh_3)_2]$ is formed as a major iron carbonyl species, which is capable of selective dehydrogenation of formic acid.

Next, we compared both catalyst solutions by IR spectroscopy. FTIR measurements were performed with a Vertex-70-FTIR spectrometer (Bruker). In Figure 10 the IR spectrum of $[Fe(CO)_3(PPh_3)_2]$ (1.5 mM) in DMF is shown.

$[Fe(CO)_3(PPh_3)_2]$ showed four contributions ν(CO) at approximately 1883, 1939, 1970, and 2048 cm^{-1}, whereas in other nonpolar solvents only one contribution ν(CO) from 1881[32a] to 1887[32b] cm^{-1} is observed. The intensities of the absorption bands are almost independent of the temperature.

For comparison of the *in situ* catalyst and the $[Fe(CO)_3(PPh_3)_2]$ complex under reaction conditions we took

(30) (a) Sowa, J. R.; Zanotti, V.; Facchin, G.; Angelici, R. J *J. Am. Chem. Soc.* **1991**, *113*, 9185. For another procedure, see also: (b) Manuel, T. A. *Inorg. Chem.* **1963**, *2*, 854. (c) Garringer, A. M.; Hesse, A. J.; Magers, R. J.; Pugh, K. R.; O'Reilly, S. A.; Wilson, A. M. *Organometallics* **2009**, *28*, 6841.

(31) Venanzi et al. reported in ^{31}P NMR experiments a singlet at 82.3 ppm for $[Fe(CO)_3(PPh_3)_2]$. Holderegger, R.; Venanzi, L. M. *Helv. Chim. Acta* **1979**, *62*, 2154.

(32) (a) Albertin, G.; Antoniutti, S.; Bortoluzzi, M. *Inorg. Chem.* **2004**, *43*, 1328. (b) Ricci, J. S.; Koetzle, T. F.; Bautista, M. T.; Hofstede, T. M.; Morris, R. H.; Sawyer, J. F. *J. Am. Chem. Soc.* **1989**, *111*, 8823. (c) Bautista, M. T.; Cappellani, E. P.; Drouin, S. D.; Morris, R. H.; Schweitzer, C. T.; Sella, A.; Zubkowski, J. *J. Am. Chem. Soc.* **1991**, *113*, 4876.

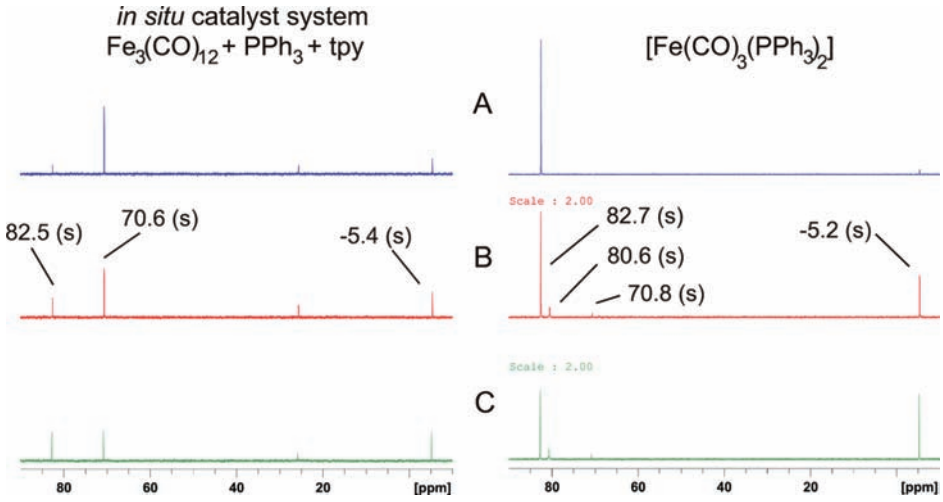

Figure 9. ^{31}P NMR spectra of the different catalyst solutions. 3 mM of the *in situ* catalyst ($Fe_3(CO)_{12}$ + 3 equiv of PPh_3 + 3 equiv of tpy) and accordingly 3 mM $[Fe(CO)_3(PPh_3)_2]$ in 10 mL of DMF; ambient pressure, 40 °C, reaction time 3 h, light irradiation via 300 W xenon lamp (385 nm cutoff via Hot Mirror). (A) 0.2 mL of $5HCO_2H \cdot 2NEt_3$ added. (B) 0.2 mL of $5HCO_2H \cdot 2NEt_3$ added and 10 min irradiation. (C) 0.2 mL of $5HCO_2H \cdot 2NEt_3$ added 30 min irradiation.

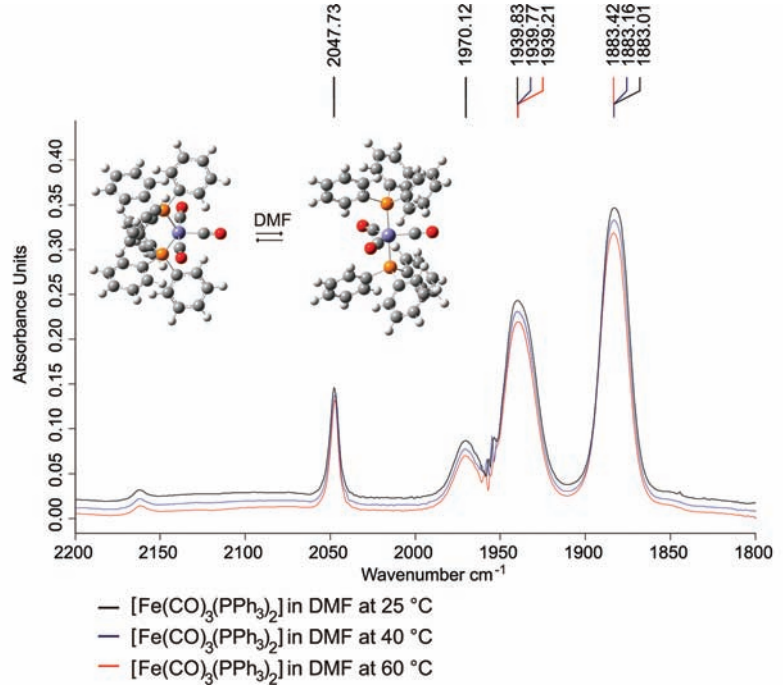

Figure 10. FT-IR spectra of 1.5 mM $[Fe(CO)_3(PPh_3)_2]$ in DMF at different temperatures. Background (DMF) subtracted. Observed absorption bands were shifted for clarity reasons.

samples from the reaction solution at defined reaction times. To obtain better quality IR spectra we decreased the amount of FA/TEA from 5 mL (standard reaction) to 0.2 mL and increased the volume of the solvent DMF from 1 to 10 mL. Except for the signal at 1883 cm^{-1}, all bands in the IR spectrum of the catalyst solution with $[Fe(CO)_3(PPh_3)_2]$ decreased dramatically under irradiation (Figure 11A). The band at 1883 cm^{-1} declined comparably less and was still seen after 180 min of irradiation. The contributions at approximately 2048, 1970, and 1943 cm^{-1} are more significant than the band at 1883 cm^{-1} in the *in situ* catalyst solution containing $Fe_3(CO)_{12}/PPh_3$/tpy without irradiation. After 30 min of constant irradiation the band at 1883 cm^{-1} increased, whereas the other bands decreased slowly. Notably, the diminishment of the bands at 2048, 1970, and 1943 cm^{-1} was significantly smaller in the *in situ* catalyst solution compared to the catalysts solution with $[Fe(CO)_3(PPh_3)_2]$, where after 180 min of irradiation only a band at 1883 cm^{-1} is observed.

To explain these spectroscopic results, we performed DFT calculations for $[Fe(CO)_3(PPh_3)_2]$. Geometry optimizations have been carried out using the Gaussian 03 program package.[33] We used the B3PW91 gradient corrected hybrid density functional[34,35] to calculate the structures and vibrational frequencies of the complexes. No imaginary frequencies were found indicating that all complexes and fragments represent at least local minimum structures on the potential energy surface. For all complexes the calculations have been performed with 6-31G* and 6-311G**

(33) Frisch, M. J. et al. *Gaussian 03*, revision D.01; Gaussian Inc.: Wallingford, CT, 2004.
(34) Becke, A. D. *J. Chem. Phys.* **1993**, *98*, 5648.
(35) Perdew, J. P.; Wang, Y. *Phys. Rev. B* **1992**, *45*, 13244.

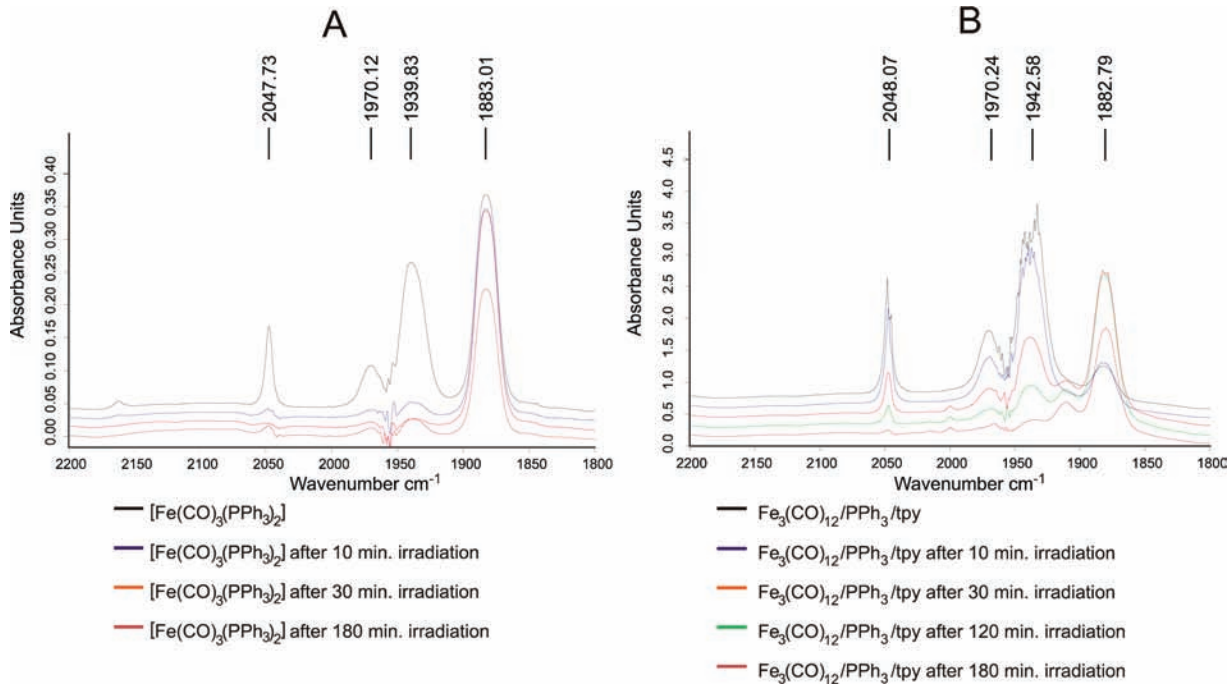

Figure 11. FT-IR spectra corresponding to different irradiation times of (A) 1.5 mM of $[Fe(CO)_3(PPh_3)_2]$ and (B) 3 mM $Fe_3(CO)_{12}$/3 equiv of PPh_3/3 equiv of tpy (Fe/PPh_3/tpy 1:1:1) in 10 mL of DMF, 0.2 mL of $5HCO_2H \cdot 2NEt_3$ added, reaction temperature 40 °C, light irradiation via 300 W xenon lamp (385 nm cutoff via hot mirror). Background (DMF) subtracted. Observed absorption bands were shifted for clarity reasons.

basis sets implemented in Gaussian 03. All calculations have been carried out on High Performance Computer Cluster in Rostock.

Figure 12 shows the optimized geometries at B3PW91/6-31G* of the complexes 18VE **1Fe** and **2Fe** and the 16VE fragments **3aFe**, **3bFe**, **4aFe**, and **4bFe** which are formed after dissociation of the ligands PPh_3 or CO from the former complexes. The metal fragments have been calculated at the singlet and triplet electronic states. The calculated geometries of complex $[Fe(CO)_3(PPh_3)_2]$ (**1Fe**) are comparable to those of Krapp et al.[36] obtained for the complex $[Fe(CO)_3(PMe_3)_2]$ by using BP86 and CCSD(T) levels of theory. In principle the bond lengths Fe−CO and Fe−P indicate the bond dissociation energies (BDE) of the ligands.

Table 3 gives the BDEs at the B3PW91/6-31G* and B3PW91/6-311G** levels of theory of the Fe−PPh_3 and Fe−CO bonds of the complexes **1Fe** and **2Fe**, respectively.

For an evaluation of our method we also calculated the optimized geometries for the iron pentacarbonyl complex (**5Fe**) and its fragments (**6aFe**, **6bFe**) and the corresponding bond dissociation energies (see Supporting Information). The results for both basis sets, 42.8 kcal mol^{-1} for 6-31G* and 41.2 kcal·mol^{-1} for 6-311G**, are in very good agreement with the experimental bond dissociation energies for $Fe(CO)_5$ (41 ± 2 kcal mol^{-1}).[37] The dissociation energies have been considered as the differences between the total energies of the complexes and the separated fragments. The dissociation energies were corrected for the zero-point energies (ZPE). For the complexes and fragments **3aFe**, **3bFe**, **4aFe**, **4bFe**, **5Fe**, and **6aFe, 6bFe** we calculated the singlet (S) as well as the triplet states (T) (see Supporting Information).[38]

For the complexes **2Fe** and **3Fe** the triplet states were lower in energy compared to the singlet state. Therefore, the dissociation energies are discussed with respect to complexes which are the lowest in energy. The dissociation of one carbonyl or phosphine ligand lead to the metal fragments **3bFe** and **4bFe** in the electronic triplet state, respectively. For both complexes **1Fe** and **2Fe** the dissociation energies of the Fe−CO bonds are lower than that for the iron pentacarbonyl complex. The displacement of one CO ligand in **1Fe** requires ~10 kcal mol^{-1} more energy than the removal of the same ligand from complex **2Fe**. However, the same trend is found for the dissociation of PPh_3 from both complexes. This behavior is nicely reflected in the measured infrared spectra (Figure 11). After irradiation complex **1Fe** is still present whereas **2Fe** lost its CO ligands. For all complexes the dissociation energy values are higher for CO compared to PPh_3. For the most stable complex **1Fe** this energy difference is ~4 kcal·mol^{-1}. Thus, the phosphine ligand will dissociate from the metal center first. The calculated frequencies are given in Table 4 for species **1Fe** and **2Fe**. For complex **1Fe** with all CO ligands in an equatorial position we obtained mainly one intensive vibrational mode at ~1990 cm^{-1}.

Complex **2Fe** yields three vibrational bands at approximately 2000, 2030, and 2090 cm^{-1}, respectively. Two contributions are significantly red-shifted versus the **1Fe** modes. These findings allow for an interpretation of the measured IR spectra before and after irradiation. Before irradiation, both complexes **1Fe** and **2Fe** are present. After irradiation, mainly the ligands of complex **2Fe** dissociate which is in agreement with the lower

(36) Krapp, A.; Pandey, K. K.; Frenking, G. *J. Am. Chem. Soc.* **2007**, *129*, 7596.
(37) Lewis, K. E.; Golden, D. M.; Smith, G. P. *J. Am. Chem. Soc.* **1984**, *106*, 3905.

(38) $[Fe(CO)_5]$ (**5Fe**) E_{tot} in kcal·mol^{-1}: −1830.043, −1830.288; ZPE /kcal·mol^{-1}: 26.6, 26.9; Bond dissociation energies D_0 /kcal·mol^{-1} (CO): 42.78, 41.20. $[Fe(CO)_4]^{(s)}$ (**6aFe**) E_{tot}:−1716.710, −1716.924; ZPE: 20.8, 20.8. $[Fe(CO)_4]^{(T)}$ (**6bFe**) E_{tot}: −1716.704, 1716.913; ZPE: 20.4, 20.1.

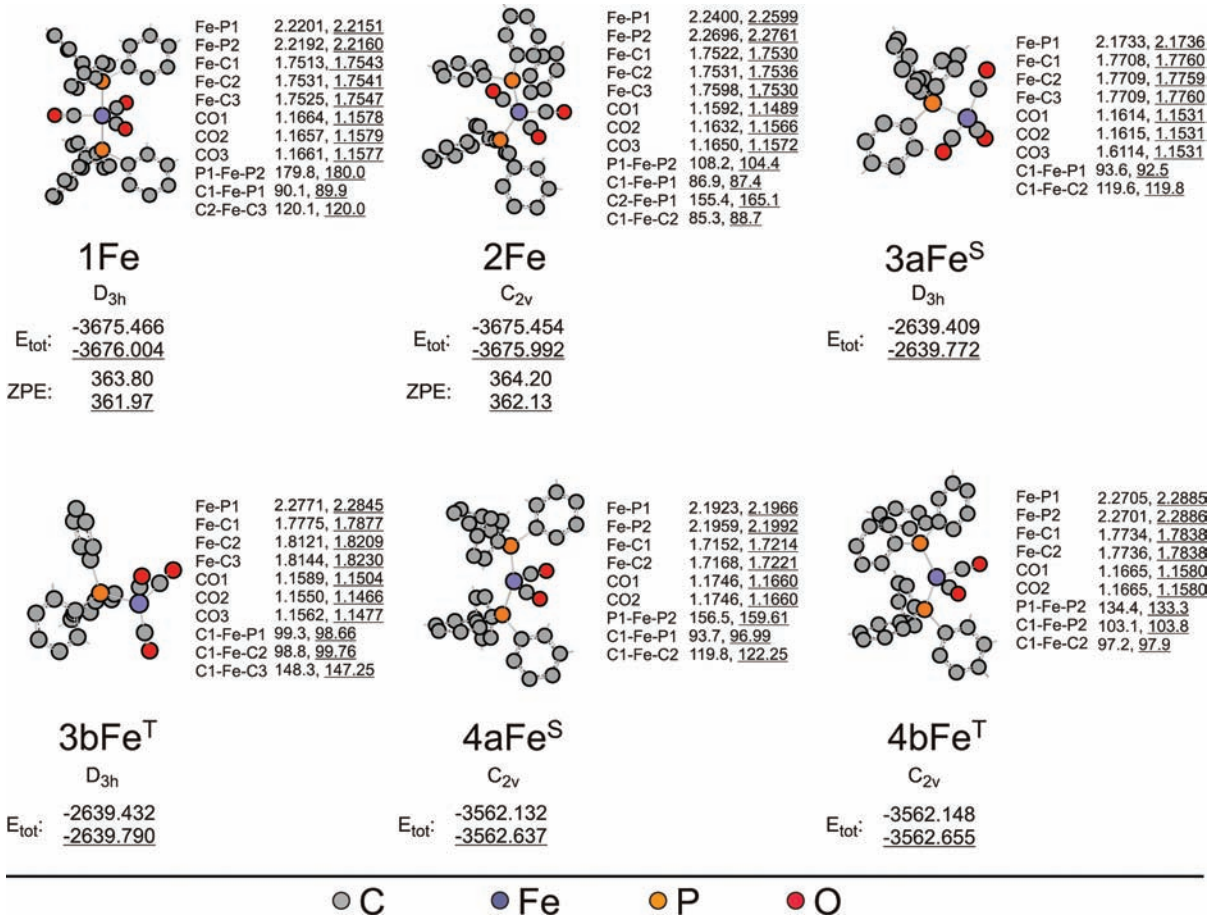

Figure 12. Optimized geometries at B3PW91/6-31G* and B3PW/6-311G** (B3PW/6-311G** values are underlined) of the calculated compounds. Calculated total energies E_{tot} and zero-point energies ZPE are given in kcal mol^{-1}. Distances in Å, angles in deg. The symmetry is given below each structure. Hydrogen atoms are omitted for clarity reasons.

Table 3. Bond Dissociation Energies D_0 of **1Fe** and **2Fe** at the B3PW91/6-31G* and B3PW/6-311G**[a] Levels of Theory

molecule	diss.	D_0 / kcal · mol^{-1}
1Fe		
	(CO)	32.53
		30.97
	(PPh_3)	28.43
		29.45
2Fe		
	(CO)	24.14
		22.86
	(PPh_3)	20.04
		21.34

[a] B3PW91/6-311G** values are underlined.

Table 4. Calculated Vibrational Frequencies ν(CO) at the B3PW91/6-31G* and B3PW/6-311G**[a] Levels of Theory for **1Fe** and **2Fe**

molecule	ν(CO) /cm^{-1}	ν(CO) /cm^{-1}	ν(CO) cm^{-1}
1Fe	2062 (0.6)	1995 (907)	1991 (894)
	2058 (0.3)	1986 (933)	1985 (938)
2Fe	2090 (1051)	2034 (323)	2007 (781)
	2089 (856)	2023 (441)	1994 (971)

[a] B3PW/6-311G** values are underlined.

bond dissociation energies for both ligands in this species. The calculated vibrational modes are ~4% larger than the measured ones, which is in agreement with the average scaling factor of 0.96 given for this level of theory.[39] For the measured vibrational band at ~2047 cm^{-1} we have no explanation yet. It also disappears after radiation and could be assigned to **2Fe**. However, compared to the other vibrational bands it appears too sharp to be related to CO vibrational modes.

Catalytic Cycle. Based on the above studies, we propose $[HFe(CO)_3(PPh_3)]^-$ as the active iron catalyst for the dehydrogenation of formic acid; however additional active iron species cannot be fully excluded. Apparently, the addition of terpyridine and similar *N*-ligands prevents rapid deactivation of the catalyst system by formation of stabilized iron complexes, which in turn can form $[HFe(CO)_3(PPh_3)]^-$ back. In this respect it is interesting to note that the IR studies confirmed less CO dissociation in the presence of terpyridine. Thus, it is likely that catalyst deactivation proceeds via CO dissociation, which is an irreversible process.

In Scheme 2, the proposed overall catalytic cycle for the iron-catalyzed hydrogen generation from formic acid is shown. The initial precatalyst, either $[Fe(CO)_3(PPh_3)_2]$ or the *in situ* mixture of $Fe_3(CO)_{12}$/terpyridine/triphenylphosphine, is activated by irradiation with visible light to give stable mononuclear iron hydride species **18**. According to the calculated dissociation energies one PPh_3 ligand dissociates from the complex to provide a free coordination site for a formate anion. Subsequent protonation via formic acid or ammonium formate and ligand exchange form the corresponding iron formate complex **19**. Release of hydrogen and recoordination of PPh_3 lead to the

(39) Merrick, J. P.; Moran, D.; Radom, L. *J. Phys. Chem.* **2007**, 11683.

Scheme 2. Proposed Catalytic Cycle for $[Fe(CO)_3(PPh_3)_2]$-Catalyzed Hydrogen Generation from Formic Acid under Light Assistance

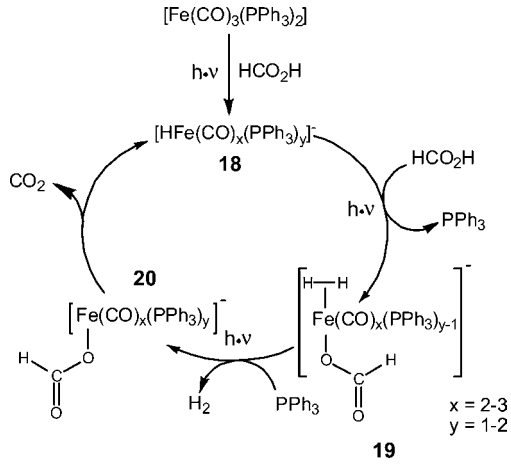

active iron complex **20**. Release of carbon dioxide through a β-hydride elimination of the coordinated formate regenerates the active catalyst **18**.

It should be noted that the release of hydrogen from the metal center is likely also influenced by light. Photoelimination reactions of molecular hydrogen from iron and ruthenium hydride species are well-known.[40] More specifically it was shown that the exited states of those metal hydride species are highly labile with respect to loss of H_2.

Conclusions

In summary, we present for the first time a light-driven iron catalyst capable of generating hydrogen from formic acid under ambient conditions. By studying the effects of various *P*- and *N*-ligands in the presence of metal carbonyl complexes, we identified active *in situ* iron catalysts consisting of $Fe_3(CO)_{12}$/PPh_3/tpy or $Fe_3(CO)_{12}$/PPh_3/phen. It is demonstrated that visible light is needed for both, creating an active system and driving the catalytic cycle. Hence, hydrogen evolution can be easily triggered by switching on and off the light source.

An overall catalyst turnover number of 126 is observed with the inexpensive and convenient combination of $Fe_3(CO)_{12}$/PPh_3/1,10-phenanthroline. Moreover, applying 6,6″-(phenyl)-2,2′:6,2″-terpyridine and PPh_3 as ligands results in a TOF of 200 h^{-1} at 60 °C. To the best of our knowledge, these are the highest activity and productivity results for a nonprecious metal based catalyst system which is capable of selectively generating hydrogen from formic acid. A detailed analysis of the catalyst solution via HRMS, NMR, and IR studies revealed that from the *in situ* catalyst mixture and molecular-defined $[Fe(CO)_3(PPh_3)_2]$ the same active species are formed which gave comparable activities. IR measurements confirmed two isomers of $[Fe(CO)_3(PPh_3)_2]$ which showed different behaviors under light irradiation. Accompanying DFT calculations revealed that under light irradiation dissociation of PPh_3 is favored compared to carbon monoxide. On the other hand loss of CO should lead to deactivation of the catalytic system, which is slowed down by the use of *N*-ligands.

(40) (a) Sweany, R. L. *J. Am. Chem. Soc.* **1981**, *103*, 2410. (b) Geoffroy, G. L.; Bradley, M. G. *Inorg. Chem.* **1977**, *16*, 744.

The use of organometallic iron complexes for catalytic reductions is yet in its infancy.[41] Apart from hydrogen generation, the reported catalyst systems are of interest for such processes, too. Due to the importance of biomimetic reductions both in biological systems and on an industrial scale, further catalyst improvements are highly desirable. In further studies we are focusing on these aspects.

Experimental Section

6,6″-(Phenyl)-2,2′:6′,2″-terpyridine. General, experimental procedure: A pressure tube equipped with a stirring bar was filled with 6.6″-dibromo-2,2′:6′,2″-terpyridine (0.1 mmol, 39.1 mg), phenylboronic acid (0.22 mmol, 26.8 mg), sodium carbonate (0.44 mmol, 47.0 mg), and $[Pd(PPh_3)_4]$ (0.005 mmol, 5.8 mg). The tube was evacuated and filled with argon. Then, dry dioxane (1 mL) and degassed water (0.2 mL) were added. The tube was closed with a Teflon screwing cap and placed in an oil bath ($T = 100$ °C). After 12 h the reaction was cooled to room temperature, and CH_2Cl_2 (5 mL) and water (5 mL) were added. The water layer was extracted an additional two times with CH_2Cl_2. The organic layers were combined and concentrated. Purification via column chromatography (eluent: cyclohexane 20:ethyl acetate 1:triethylamine 0.2) yielded the phenyl-substituted terpyridine (0.095 mmol, 36.6 mg, 95%) as a white, crystalline solid. ^{1}H NMR ($CDCl_3$): $\delta = 8.66$ (1, d, $J = 7.8$ Hz), 8.63 (2, dd, $J = 7.8$, 0.9 Hz), 8.12−8.09 (8, m), 7.97 (4, t, $J = 15.6$ Hz), 7.87 (3, t, $J = 7.8$ Hz), 7.73 (5, dd, $J = 7.8$, 0.9 Hz), 7.48−7.35 (6,7 m) ppm; ^{13}C NMR ($CDCl_3$): $\delta = 156.5$ (Cq), 155.6 (Cq), 155.2 (Cq), 139.3 (Cq), 138.2 (CH), 137.8 (CH), 129.1 (CH), 128.8 (CH), 127.0 (CH), 121.4 (CH), 120.5 CH), 119.6 (CH) ppm. FTIR (ATR) 3052.6, 2922, 1564, 1427, 1265.7, 1089.7, 1022.6, 988.5, 803.3, 760.3, 693.8, 634.9 cm^{-1}; HRMS (ESI-TOF) *m/z* calcd for $C_{27}H_{20}N_3$ + H 386.1652, found 386.1653.

6,6″-(2-Methylphenyl)-2,2′:6′,2″-terpyridine. General, experimental procedure: A pressure tube equipped with a stirring bar was filled with 6.6″-dibromo-2,2′:6′,2″-terpyridine (0.1 mmol, 39.1 mg), 2-methylphenylboronic acid (0.22 mmol, 29.9 mg), sodium carbonate (0.44 mmol, 47.0 mg), and $[Pd(PPh_3)_4]$ (0.005 mmol, 5.8 mg). The tube was evacuated and filled with argon. Then, dry dioxane (1 mL) and degassed water (0.2 mL) were added. The tube was closed with a Teflon screwing cap and placed in an oil bath ($T = 100$ °C). After 12 h the reaction was cooled to room temperature, and CH_2Cl_2 (5 mL) and water (5 mL) were added. The water layer was extracted an additional two times with CH_2Cl_2. The organic layers were combined and concentrated. Purification via column chromatography (eluent: cyclohexane 20:ethyl acetate 1:triethylamine 0.2) yielded the 2-methylphenyl-substituted terpyridine (0.080 mmol, 33.1 mg, 80%) as a white, crystalline solid. ^{1}H NMR ($CDCl_3$): $\delta = 8.54$ (2, dd, $J = 7.9$, 1.0 Hz), 8.46 (1, d, $J = 7.8$ Hz), 7.88−7.81 (3,6 m), 7.46−7.43 (4, m), 7.38 (3, dd, $J = 7.7$, 1.0 Hz), 7.27−7.22 (7,8,9 m), 2.43 (s, CH_3) ppm; ^{13}C NMR ($CDCl_3$): $\delta = 159.4$ (Cq), 155.3 (Cq), 155.3 (Cq), 140.3 (Cq), 138.2 (CH), 138.0 (CH), 137.3 (CH), 136.2 (Cq), 131.0 (CH), 129.9 (CH), 128.4 (CH), 126.0 (CH), 124.2 (CH), 121.4 (CH), 119.0 (CH), 20.8 (CH_3) ppm. FTIR (ATR) 3052.6, 2922, 1564, 1427, 1265.7, 1155.6,

(41) For recent applications of iron-catalyzed hydrogenations and transfer hydrogenations, see: (a) Enthaler, S.; Erre, G.; Tse, M. K.; Junge, K.; Beller, M. *Tetrahedron Lett.* **2006**, *47*, 8095. (b) Enthaler, S.; Hagemann, B.; Erre, G.; Junge, K.; Beller, M. *Chem. Asian J.* **2006**, *1*, 598. (c) Sylvester, K. T.; Chirik, P. J. *J. Am. Chem. Soc.* **2009**, *131*, 8772. (d) Trovitch, R. J.; Lobkovsky, E.; Bill, E.; Chirik, P. J. *Organometallics* **2008**, *27*, 1470. (e) Casey, C. P.; Guan, H. *J. Am. Chem. Soc.* **2009**, *131*, 2499. (f) Casey, C. P.; Guan, H. *J. Am. Chem. Soc.* **2007**, *129*, 5816. (g) Lagaditis, P. O.; Mikhailine, A. A.; Lough, A. J.; Morris, R. H. *Inorg. Chem.* **2010**, *49*, 1094. (h) Morris, R. H. *Chem. Soc. Rev.* **2009**, *38*, 2282. (i) Mikhailine, A. A.; Lough, A. J.; Morris, R. H. *J. Am. Chem. Soc.* **2009**, *131*, 1394. (j) Meyer, N.; Lough, A. J.; Morris, R. H. *Chem.—Eur. J.* **2009**, *15*, 5605. (k) Sui-Seng, C.; Freutel, F.; Lough, A. J.; Morris, R. H. *Angew. Chem., Int. Ed.* **2008**, *47*, 940.

1075.1, 1022.6, 988.5, 803.3, 760.3, 693.8, 634.9 cm^{-1}; HRMS (ESI-TOF) *m*/*z* calcd for $C_{29}H_{24}N_3$ + H 414.1965, found 414.1967.

$Fe(CO)_3(PPh_3)_2$. General, experimental procedure: A double walled reaction vessel equipped with a stirring bar was purged with argon to remove all other gases. It was filled with benzylidenacetonetricarbonyliron (2.1 mmol, 0.6 g), triphenylphosphine (4.6 mmol, 1.21 g), and 20 mL of toluene. The vessel was closed and connected to a thermostate and was maintained at 60 °C for 16 h. The reaction mixture was cooled to room temperature, and the solution was reduced to 3 mL. *N*-Hexane (10 mL) was added, and the solution was kept at −30 °C for 16 h. The resulting yellow precipitate was filtered and washed (3 × 2 mL *n*-hexane; 3 × 2 mL diethylether) while excluding air. The bright yellow crystals were dried under reduced pressure. Resulting yield: 1.85 mmol, 1.23 g, 88%. ^1H NMR ($CDCl_3$): δ = 7.3−7.6 (m, Ph) ppm; ^{31}P NMR ($CDCl_3$): δ = 82.9 (PPh_3) ppm; FTIR (ATR) ν(CO) 1881 (s), cm^{-1}; HRMS (ESI-TOF) *m*/*z* calcd for $C_{29}H_{24}N_3$ + H 664.1014, found 664.1022.

Acknowledgment. This work has been supported by the state of Mecklenburg-Vorpommern, BMBF, and DFG (Leibniz prize and GRK1213). We thank D. Mellmann, A. Koch, S. Buchholz, C. Fischer, A. Lehmann, A. Kammer, and K. Mevius for their excellent analytical and technical support. F.G. thanks the Fonds der Chemischen Industrie (FCI) for a Kekulé grant.

Supporting Information Available: Complete refs 8b, 33; experimental data; ^1H NMR data for all new compounds; and computational details. This material is available free of charge via the Internet at http://pubs.acs.org.

JA100925N